



저작자표시-비영리-변경금지 2.0 대한민국

이용자는 아래의 조건을 따르는 경우에 한하여 자유롭게

- 이 저작물을 복제, 배포, 전송, 전시, 공연 및 방송할 수 있습니다.

다음과 같은 조건을 따라야 합니다:



저작자표시. 귀하는 원저작자를 표시하여야 합니다.



비영리. 귀하는 이 저작물을 영리 목적으로 이용할 수 없습니다.



변경금지. 귀하는 이 저작물을 개작, 변형 또는 가공할 수 없습니다.

- 귀하는, 이 저작물의 재이용이나 배포의 경우, 이 저작물에 적용된 이용허락조건을 명확하게 나타내어야 합니다.
- 저작권자로부터 별도의 허가를 받으면 이러한 조건들은 적용되지 않습니다.

저작권법에 따른 이용자의 권리는 위의 내용에 의하여 영향을 받지 않습니다.

이것은 [이용허락규약\(Legal Code\)](#)을 이해하기 쉽게 요약한 것입니다.

[Disclaimer](#)

공학석사학위논문

광학 계측법을 이용한 서브옥탄
가솔린과 바이오 에탄올/부탄올
혼합 연료의 GDI 분사 특성 연구

Analysis of the Effect of Ethanol and Butanol Addition
to Sub-octane Gasoline on GDI Spray Characteristics
by Optical Visualization

2019 년 2 월

서울대학교 대학원

기계항공공학부

민 형 은

광학 계측법을 이용한 서브옥탄 가솔린과 바이오 에탄올/부탄올 혼합 연료의 GDI 분사 특성 연구

Analysis of the Effect of Ethanol and Butanol Addition
to Sub-octane Gasoline on GDI Spray Characteristics
by Optical Visualization

지도교수 송 한 호

이 논문을 공학석사 학위논문으로 제출함

2018 년 10 월

서울대학교 대학원

기계항공공학부

민 형 은

민형은의 공학석사 학위논문을 인준함

2018 년 12 월

위 원 장

민 경 덕



부위원장

송 한 호



위 원

고 승 한



Abstract

Analysis of the Effect of Ethanol and Butanol Addition to Sub-octane Gasoline on GDI Spray Characteristics by Optical Visualization

Hyungeun Min

Department of Mechanical & Aerospace Engineering

The Graduate School

Seoul National University

Blending biofuels with gasoline has been suggested as the way to decarbonize the transport section and to increase octane number. In this study, the spray characteristics of sub-octane gasoline and bio-ethanol/bio-butanol (7:3) blended fuel was derived in the background conditions of real GDI engine by using a constant volume chamber. The behavior of spray was measured by Mie-scattering and Schlieren photography method. Various bio-alcohol concentration fuels (EB 0, 6, 15, 30, 60, 88) were tested in the background conditions corresponded to the engine operating conditions. As a result, the operating range of the GDI engine included in the transition region in

terms of flash-boiling, so the spray geometry changes most actively by flash-boiling. The flash-boiling occurred most strongly with the EB30 mixture due to vapor pressure and boiling point change of fuel according to the evaporation ratio. However, the effects of bio-alcohol concentration and flash-boiling on penetration length and projected area were different according to the background pressure and temperature due to the formation of a single plume in the region where flare-flashing occurs.

Keywords: Bio-alcohol, Bio-blended fuel, GDI spray characteristics,
Flash-boiling, Mie-scattering

Student Number: 2014-21850

Abstract	_____	i
Contents	_____	iii
List of Tables	_____	v
List of Figures	_____	vi
1. Introduction	_____	1
1.1 Research background	_____	1
1.2 Previous research	_____	2
1.3 Research objective	_____	3
2. Experimental Setup	_____	9
2.1 Constant volume chamber	_____	9
2.2 Injection system	_____	9
2.3 Spray visualization method	_____	10
3. Experimental Conditions	_____	14
3.1 Fuel conditions	_____	14
3.2 Background conditions	_____	14
3.3 Injection conditions	_____	15
4. Experimental Results	_____	20
4.1 Comparison of the Schlieren and Mie-scattering	_____	20
4.2 Flash-boiling according to the background conditions	_____	20
4.3 Spray characteristics according to the bio-alcohol concentration	_____	29
4.3.1 Results at low background temperature and pressure	_____	37
4.3.2 Results at middle background temperature and pressure	_____	37
4.3.3 Results at high background temperature and pressure	_____	38
5. Conclusion	_____	42

References	_____	43
Abstract (in Korean)	_____	45

List of Tables

- | | |
|-----------|--|
| Table 1.1 | Renewable transport mandates at the national levels |
| Table 1.2 | Properties of sub-octane gasoline, bio-ethanol, and bio-butanol used in this study |
| Table 2.1 | Detailed specification of the constant volume chamber |
| Table 3.1 | Fuel conditions for experiments |
| Table 3.2 | GDI engine driving condition to simulate |
| Table 3.3 | Summary of experimental conditions |

List of Figures

- Figure 1.1 Global energy-related CO₂ emissions by sector
- Figure 1.2 GHG emissions reduction potential for biofuels
- Life cycle analysis
- Figure 2.1 The overall experimental setup
- Figure 2.2 The experimental setup and sample images of Schlieren photography
- Figure 2.3 The experimental setup and sample images of Mie-scattering
- Figure 3.1 Internal temperature and pressure of the GDI engine at injection timing
- Figure 3.2 Injection pressure of the GDI engine at each driving conditions
- Figure 4.1 Comparison of Schlieren photography and Mie-scattering results
- Figure 4.2 Comparison of penetration length and spray angle from Schlieren photography and Mie-scattering
- Figure 4.3 Spray images of EB 0 and EB 88 according to the background conditions (@ aSOI 0.7 ms)
- Figure 4.4 Flash-boiling process in PT diagram
- Figure 4.5 Flash-boiling process
- Figure 4.6 Vapor pressure of sub-octane gasoline, bio-ethanol, and bio-butanol according to temperature
- Figure 4.7 Macroscopic spray structure and vapor quantity for

flash-boiling sprays

- Figure 4.8 Velocity field around the flash-boiling sprays
- Figure 4.9 Spray images at engine operating conditions according to the bio-alcohol concentration (@ aSOI 0.7 ms)
- Figure 4.10 (a) Vapor pressure of ethanol blend in gasoline with different relative proportions of ethanol by reference [10], (b) Vapor pressure of tested fuel measured by K-Petro (at 37.8 °C)
- Figure 4.11 Boiling temperature according to the distilled ratio of each fuel
- Figure 4.12 10 % and 50 % distilled point according to the alcohol concentration
- Figure 4.13 Predicted distillation curves for blends of ethanol and gasoline with non-ideal mixtures
- Figure 4.14 Penetration length and projected area of spray at background condition of 30 °C and 0.2 bar
- Figure 4.15 Penetration length and projected area of spray at background condition of 55 °C and 0.4 bar
- Figure 4.16 Penetration length and projected area of spray at background condition of 80 °C and 0.6 bar

1. Introduction

1.1. Research background

In recent years, environmental problems have arisen due to the greenhouse gas and exhaust emissions such as NO_x and PM from the use of fossil fuels. In addition, the problem of depletion due to the continuous use of fossil fuels is emerging, so many attempts have been made to solve these problems. In particular, as shown in Figure 1.1, carbon dioxide emissions are increasing at a rapid pace, and it is known that the transport sector accounts for a fairly large proportion of them [1]. Therefore, blending biofuels with conventional fossil fuels was suggested as one way to decarbonize the transport sector. It is considered to use biodiesel to replace diesel, and to use bio-ethanol or bio-butanol to replace gasoline. According to previous study of life cycle analysis, greenhouse gas emissions decrease as biofuels are used as shown in Figure 1.2 [2].

In an effort to increase biofuel usage, many countries, including the United States, have set mandatory blending ratios of biodiesel and ethanol as shown in Table 1.1 [3]. In Korea, the Renewable Fuel Standard (RFS) has been implemented since 2015 to reduce dependence on petroleum resources, and the mandatory blending ratios of biodiesel has been raised from 2.5 % to 3 % this year. However, since there is no standard for bio-alcohol blending for gasoline, various agencies gathered to carry out the energy technology

development program, study on development of optimization for domestic application improvement of E3 level transport biofuels. In this project infrastructure technology to use bio-ethanol and bio-butanol in domestic SI engines has been developed. This study has also been conducted as a basic study to apply bio-alcohol blended fuel to GDI engines.

1.2. Previous research

In the case of the bio-alcohol, it was mainly used as a gasoline additive fuel because it can reduce the amount of greenhouse gas emission as a carbon neutral, oxygen-containing fuel and also can increase the octane number. Also, it is expected that the characteristics of oxygen-containing fuels can improve the problems of PM generation, which is frequently occurring in direct injection spark ignition engines.

In a GDI engine, combustion occurs after the fuel is directly injected into the cylinder, so the injection characteristic is important for the fuel evaporation and mixing process. However, bio-alcohol was expected to have different fuel injection and evaporation characteristics because of difference in various properties such as vapor pressure, density, and heat of vaporization compared with conventional gasoline, which can be a problem in direct injection spark ignition engines.

Previous researches have compared the spray characteristics of

ethanol and butanol with those of gasoline when they used as a single component fuel [4]. In the case of gasoline and ethanol blended fuels, currently used in other countries, the spray characteristics were analyzed up to the mixing ratio of high concentration [5]. However, few studies have analyzed the spray characteristics of gasoline mixed with ethanol as well as butanol.

1.3. Research objective

In this study, the spray characteristics of sub-octane gasoline and bio-ethanol/butanol blended fuel was investigated in background conditions of real GDI engine by optical visualization. Considering the fuel characteristics such as octane number, vapor pressure and phase separation characteristics of bio-alcohol, we aimed to blend ethanol and butanol in a ratio of 7 to 3. The properties of sub-octane gasoline and bio-alcohol used in this study are shown in Table 1.2. The octane number of sub-octane gasoline is 90, but the octane number of bio-ethanol and bio-butanol is as high as 111 and 100, respectively, so bio-alcohol can act as an octane booster in the sub-octane gasoline. However, since ethanol has a low vapor pressure of 15 kPa, and butanol also has a very low vapor pressure of 1.6 kPa, it is expected that the characteristics of vaporization and mixing will change significantly. Therefore, the composition ratio of ethanol and butanol was fixed at 7 to 3, and the spray characteristics were analyzed under GDI engine conditions using constant volume chamber

while increasing the total alcohol content in the sub-octane gasoline. The behavior of spray was measured by optical visualization such as Mie-scattering and Schlieren photography method, and various bio-alcohol concentration fuels (EB 0, 6, 15, 30, 60, 88) were tested.

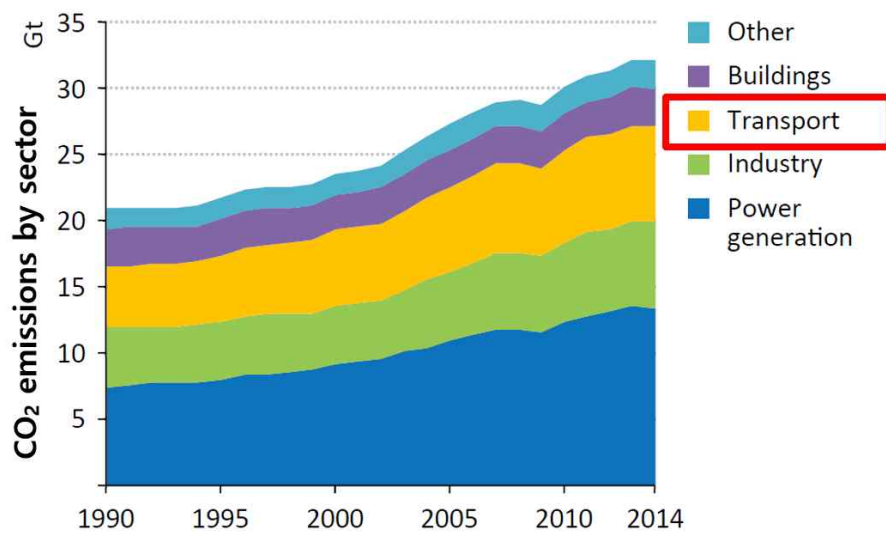


Figure 1.1 Global energy-related CO₂ emissions by sector [1]

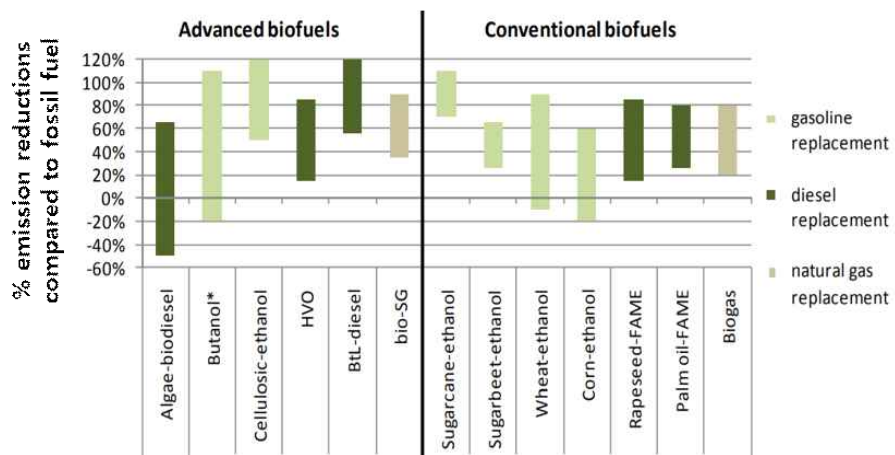


Figure 1.2 GHG emissions reduction potential for biofuels
 - Life cycle analysis [2]

Table 1.1 Renewable transport mandates at the national levels [3]

Country	Biofuel Blend Mandates		
	Existing biodiesel blend mandate (% biodiesel)	Existing ethanol blend mandate (% ethanol)	Biofuel mandate by future year
United States			Renewable Fuel Standard(RFS) 2018 standards: 68.6 billion liters total renewable fuels
Hawaii, Missouri and Montana	-	10	
Minnesota	10	10	B20 by 2019
Louisiana	2	2	
China	1 (in Taipei)	10 (in 9 provinces)	
Brazil	8	27	B10 by 2019
India	15	22.5	
South Korea	3	-	

Table 1.2 Properties of sub-octane gasoline, bio-ethanol,
and bio-butanol used in this study

Evaluation parameter		Sub-octane gasoline	Bio-ethanol	Bio-butanol
Octane number		90	111	100
Vapor pressure (37.8°C, kPa)		52.7	15	1.6
Boiling point(°C)		58.1	77	115.4
Oxygen content(wt%)		< 0.1	35.3	21.6
Element	H(m/m %)	14.3	13.1	13.6
	C(m/m %)	85.7	52.1	64.9
Calorific value(MJ/kg)		46.57	29.24	36
Density (15°C, g/cm ³)		0.729	0.803	0.814

2. Experimental Setup

2.1. Constant volume chamber

In this study, the constant volume chamber was used to analyze the characteristics of the spray according to the bio-alcohol concentration. The chamber can simulate the internal temperature and pressure with the GDI engine operating conditions. The temperature of the chamber can be controlled using the system consisting of jacket type heater and chiller, and the pressure inside the chamber can be controlled with vacuum and pressurized pumps. In addition, the four quartz windows of the chamber enable the spray visualization. The detailed specification of the chamber can be seen in Table 2.1.

2.2. Injection system

For injection of the bio-blended fuels, the GDI injector and fuel compression system were adapted. The injector was adopted by the 6 hole GDI injector of the Continental Corporation. The fuel compression system was constructed based on a Haskel pump, and a DSPACE power module was used for injector driving. The fuel pressure was controlled by using common rail and PCV rail driver. The overall experimental system can be seen in Figure 2.1.

2.3. Spray visualization method

For optical visualization of the fuel spray, the Schlieren photography method and Mie-scattering method were applied. Schlieren photography is a method of measuring shadows through the phenomenon of refraction of light according to a density gradient, allowing observation of the gas field. Mie-scattering, on the other hand, can observe the liquid areas by measuring light scattered by fuel droplets. In addition, a high-speed camera was used to observe the spray shape changing with time in 0.1 ms increments. The experimental setup and sample images of Schlieren photography and Mie-scattering can be seen in Figure 2.2 and Figure 2.3.

Table 2.1 Detailed specification of the constant volume chamber

Max. Pressure	150 bar
Max. Temperature	2000 K
Dimension (mm ³)	220 * 220 * 220
Optical Windows	4 ea. (Quartz)
Fan Type	Magnetic drive

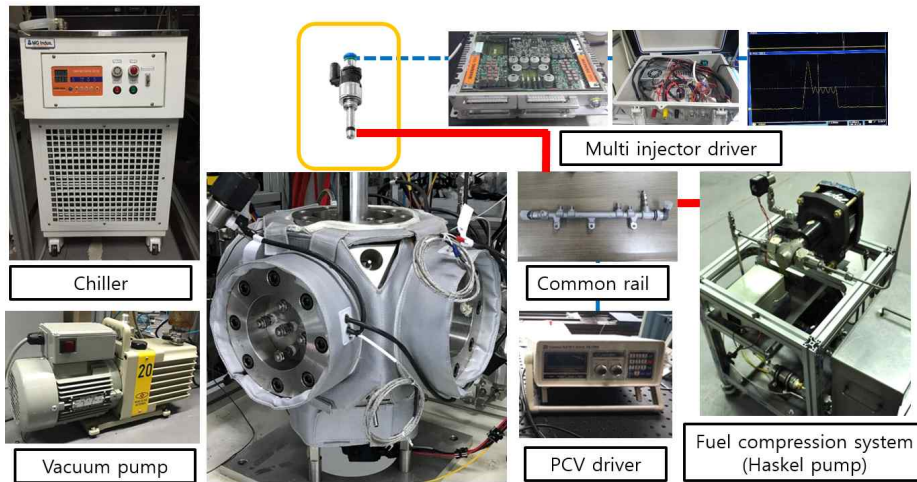


Figure 2.1 The overall experimental setup

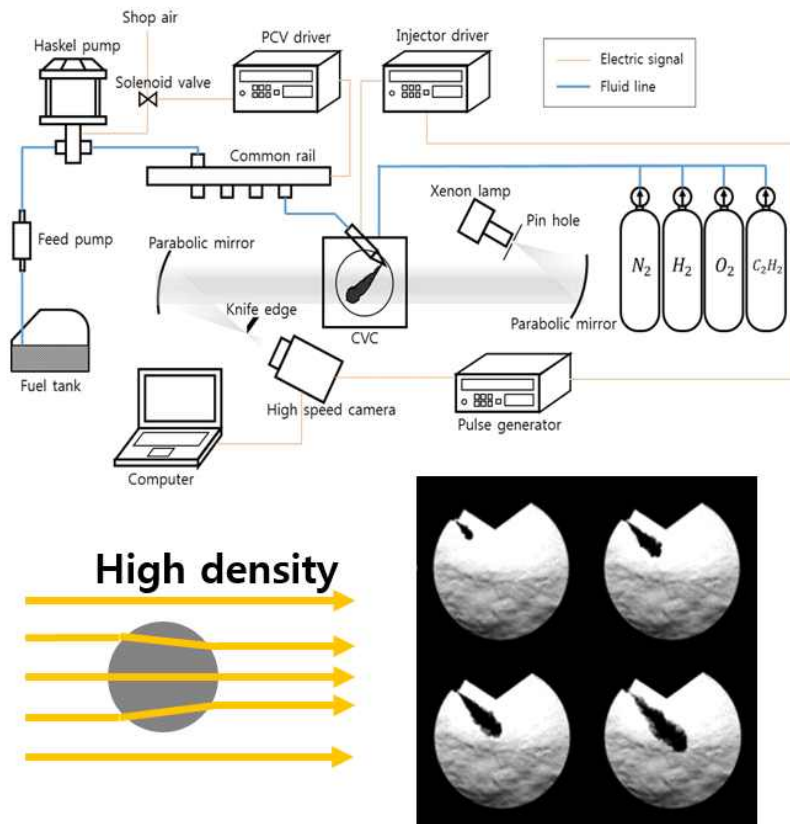


Figure 2.2 The experimental setup and sample images of Schlieren photography

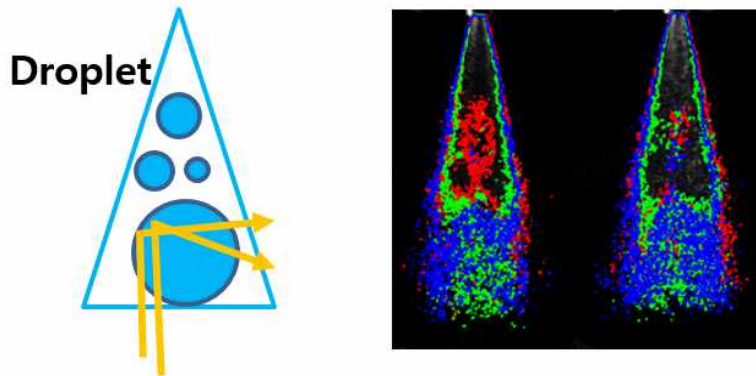
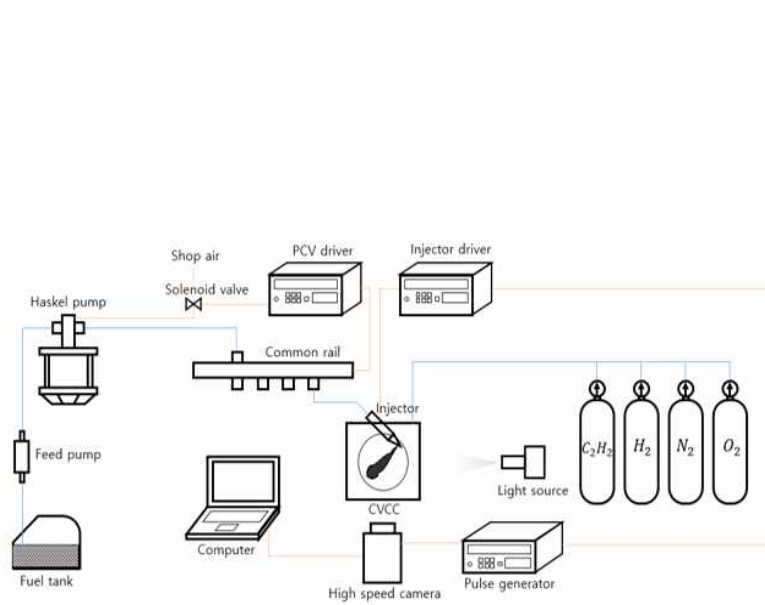


Figure 2.3 The experimental setup and sample images of Mie-scattering

3. Experimental Conditions

3.1. Fuel conditions

In this study, 6 kinds of bio-blended fuels by alcohol content was tested. As shown in Table 3.1, we tested from EB 0, pure sub-octane gasoline with 0 % bio-alcohol, to EB 88 with 100 % bio-alcohol. The mixing ratio of ethanol and butanol in all fuels was fixed at 7 to 3. The name of fuel was set so that the concentration of oxygen contained in the fuels is the same as the concentration when ethanol is only mixed. For example, the oxygen concentration of the EB 30 fuel was the same as the oxygen concentration of 30 % ethanol + 70 % sub-octane gasoline. The reason for this number in fuel name is that biofuel mixing standards are defined as the oxygen concentration in the fuel in many countries.

3.2. Background conditions

The background conditions of the constant volume chamber for injection were determined based on the real GDI engine driving conditions performed with the Hyundai 2.4 L thetaII engine. A broad background temperature and pressure conditions were taken to cover the GDI engine operating conditions of BMEP at 2 to 6 bar and 1500 to 2500 RPM as shown in Table 3.2. From the engine test results, as shown in Figure 3.1, the internal temperature of the engine at

injection timing increased from 30 to 90 degrees Celsius, while the background pressure increased from 0.2 bar to 0.6 bar depending on the engine load and operating speed. For that reason, the injection experiments were conducted at three different temperature and three different pressure as shown in Figure 3.1.

3.3. Injection conditions

Figure 3.2 shows the injection pressure of the GDI engine at each engine driving condition. The injection pressure to investigate the spray characteristics was determined to 50 bar and 70 bar based on the actual engine measurement results. The final experimental conditions are summarized in Table 3.3. In summary, the experiment was carried out under 216 conditions according to fuels, background conditions, injection pressures, and optical measurement techniques.

Table 3.1 Fuel conditions for experiments

Fuel name	Fuel composition	SUB (% vol.)	Ethanol (% vol.)	Butanol (% vol.)	Oxygen (wt %)
EB0	SUB	100	0	0	<0.1
EB6	SUB + E:B (70:30)	93.6	4.5	1.9	2.3
EB15	SUB + E:B (70:30)	83.3	11.6	5.1	5.7
EB30	SUB + E:B (70:30)	66.6	23.3	10.1	11.3
EB60	SUB + E:B (70:30)	31.8	47.8	20.5	22.6
EB88	E:B (70:30)	0	70	30	33.1

Table 3.2 GDI engine driving condition to simulate

Engine driving condition	RPM	BMEP (bar)
1	1500	2
2		4
3		6
4	2000	2
5		4
6		6
7	2500	2
8		4
9		6

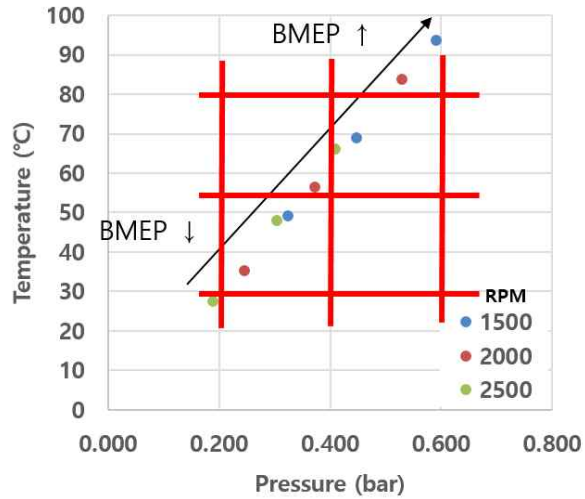


Figure 3.1 Internal temperature and pressure of the GDI engine at injection timing

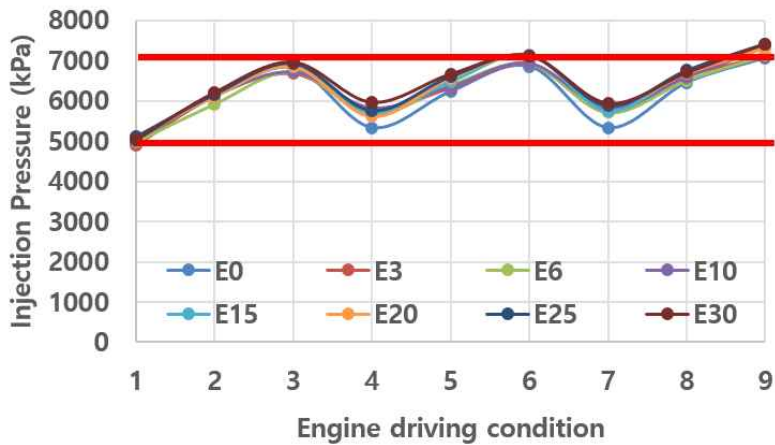


Figure 3.2 Injection pressure of the GDI engine at each driving conditions

Table 3.3 Summary of experimental conditions

Fuel	Background temperature	Background pressure	Injection pressure	Diagnostics
EB0				
EB6	30 °C	0.2 bar	50 bar	Schlieren
EB15	55 °C	0.4 bar	70 bar	Mie-scattering
EB30	80 °C	0.6 bar		
EB60				
EB88				

4. Experimental Results

4.1. Comparison of the Schlieren and Mie-scattering

Figure 4.1 shows the results of Schlieren and Mie-scattering measurements of the EB 0 (Sub-octane gasoline 100%) fuel according to the background conditions. Generally, the Schlieren region, which measures the gas region, is wider than the Mie region, which senses droplets. However, since the intensity of the light source for Mie-scattering is very strong in this study, the Mie region is almost similar to the Schlieren region as shown in Figure 4.2. In addition, the Mie-scattering image was clearer due to the high sensitivity, so the image from Mie-scattering which can measure micrometer-sized droplets was mainly used for analysis in this study.

4.2. Flash-boiling according to the background conditions

The spray images of the EB 0 and EB 88 (Alcohol 100 %) according to the background conditions are depicted in Figure 4.3. The shape of the spray changes significantly due to the flash-boiling effect according to the background conditions. Flash-boiling is a phenomenon that occurs when a sub-cooled liquid is decompressed very quickly until it is much lower than the saturation pressure as shown in Figure 4.4 [6]. When the liquid fuel is exposed to

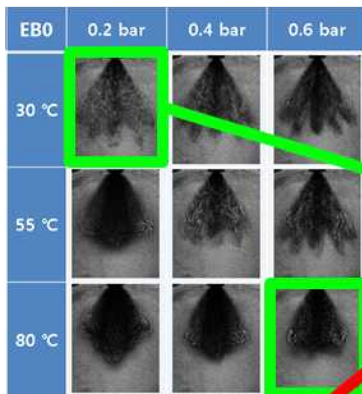
sub-saturation pressure, the bubble nucleation step is initiated. In this step, a portion of the liquid becomes a vapor forming bubbles within the liquid, and these bubbles expand rapidly while the fuel is injected. As these steps progress, bubble breakup eventually occurs, and the fuel droplet is atomized into a very small size as shown in Figure 4.5 [7].

In this study, the background temperature and pressure conditions of the experiments included the front and back boundaries of the flash-boiling. The specific boundary changes depending on the bio-alcohol content as shown in Figure 4.6. In that reason, the flash-boiling phenomenon occurred and becomes stronger as the background temperature increases or the background pressure decreases. Therefore, according to the degree of flash-boiling, the experimental region was divided into the non-flash-boiling region, transition region, and flare flashing region, and it was also indicated in Figure 4.3. Particularly, the real engine operating conditions corresponds to the transition region changing from non-flash-boiling state to flash-boiling state.

Figure 4.7 gives an overview of the macroscopic spray structure and the quantitative characteristics such as penetration and plume width of the spray in each region [8]. The shape of the spray depends on the degree of flash-boiling because flash-boiling produces vortices that push the plumes toward the central axis as shown in Figure 4.8 [9]. When flash-boiling begins, these vortices start to gather the plumes into the center, and the boundary of the plume

becomes blurred. Therefore, the axial velocity of fuel droplets decreases, and the penetration length of the spray becomes shorter. Then, when it goes to the flare flashing region, each plume is completely merged to form a single plume, so penetration gradually increases again.

Schlieren photography



Mie scattering

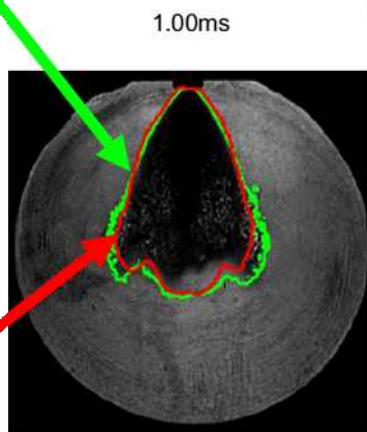
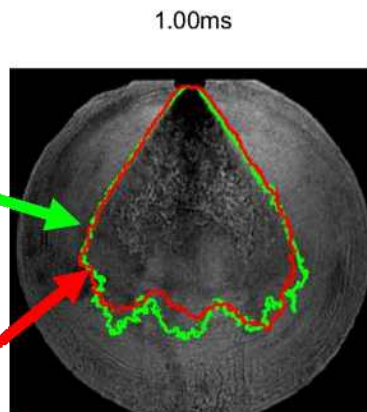
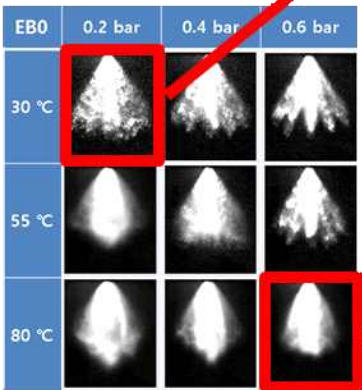


Figure 4.1 Comparison of Schlieren photography and Mie-scattering results

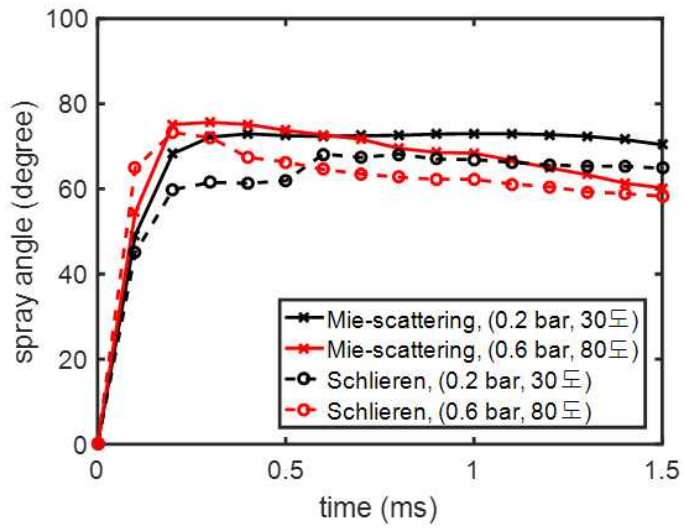
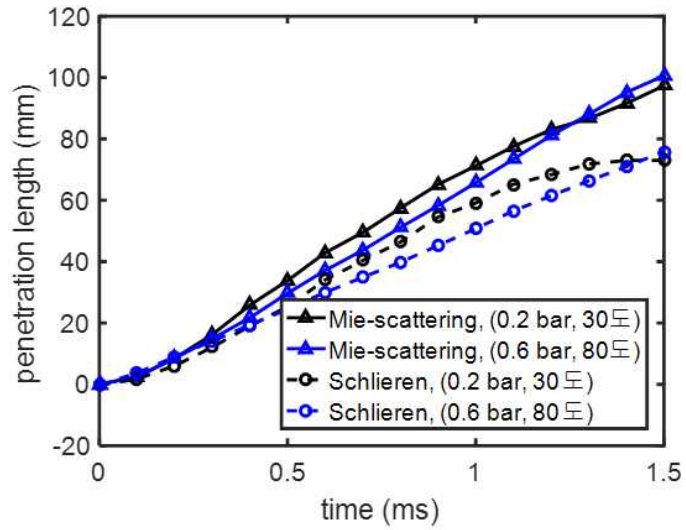


Figure 4.2 Comparison of penetration length and spray angle from Schlieren photography and Mie-scattering

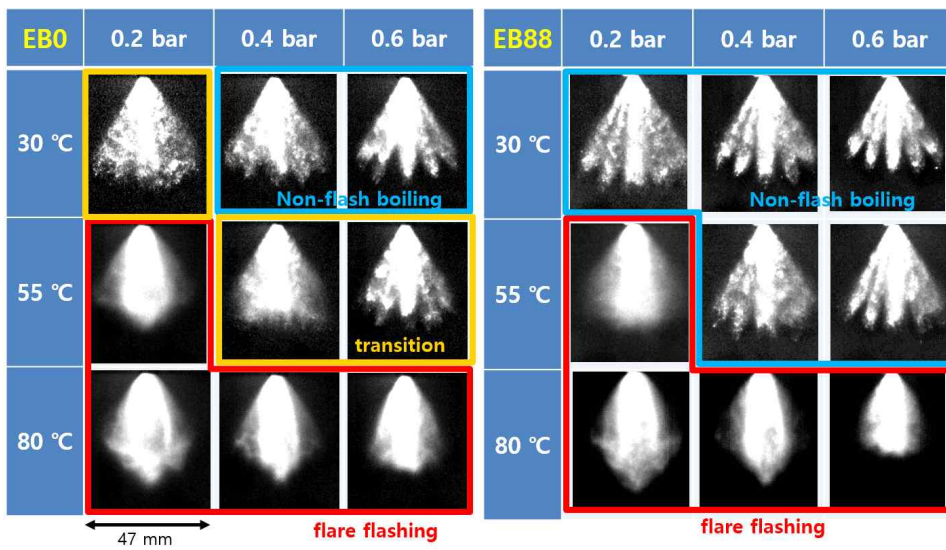


Figure 4.3 Spray images of EB 0 and EB 88 according to the background conditions (@ aSOI 0.7 ms)

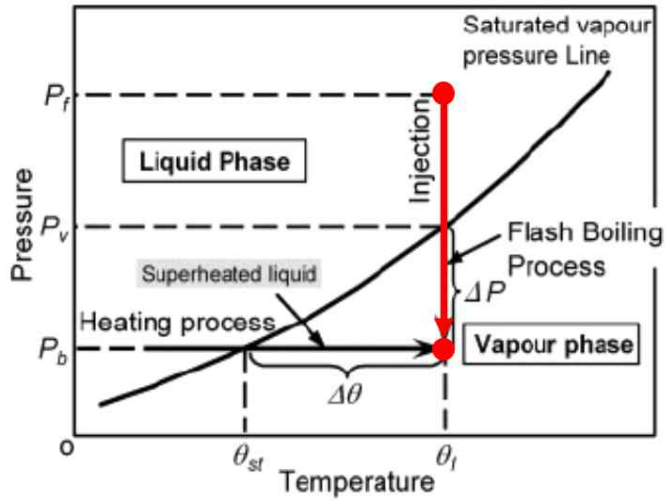


Figure 4.4 Flash-boiling process in PT diagram [6]

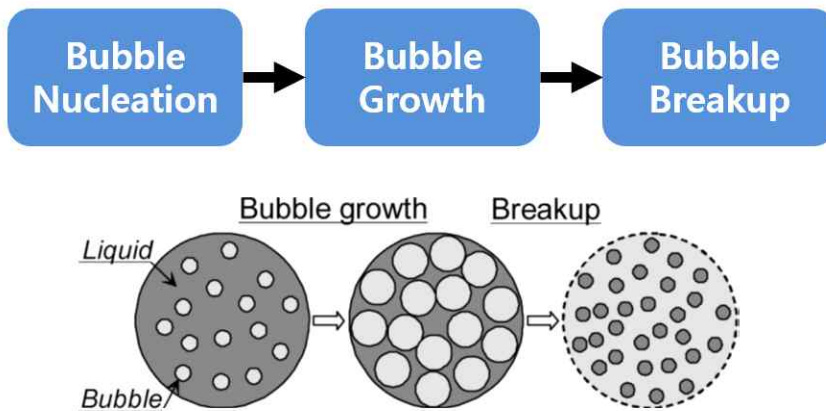


Figure 4.5 Flash-boiling process [7]

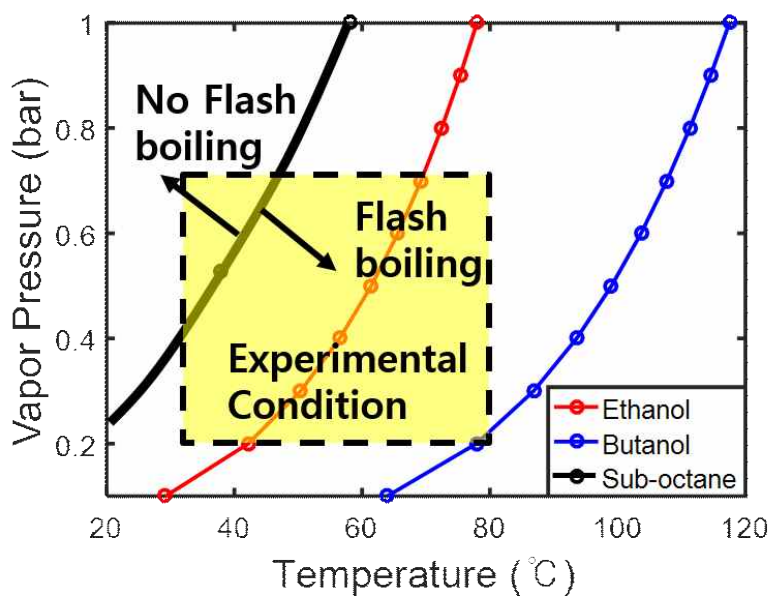


Figure 4.6 Vapor pressure of sub-octane gasoline, bio-ethanol, and bio-butanol according to temperature

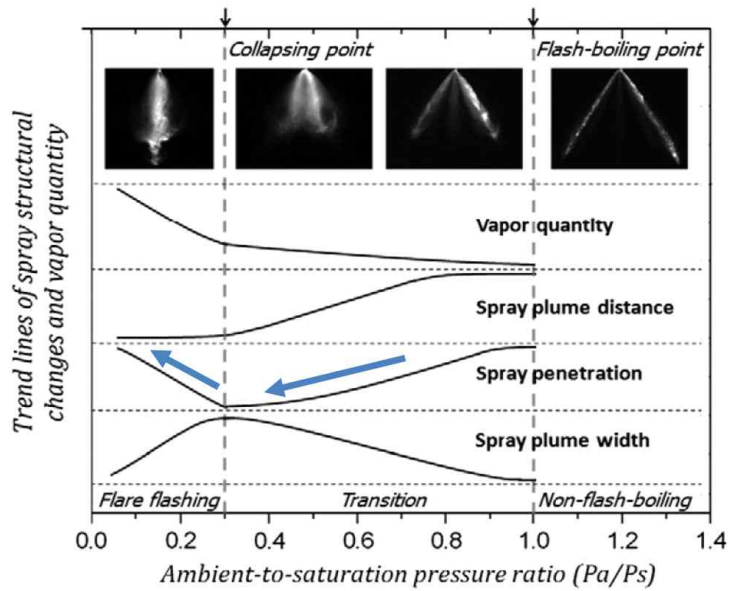


Figure 4.7 Macroscopic spray structure and vapor quantity for flash-boiling sprays [8]

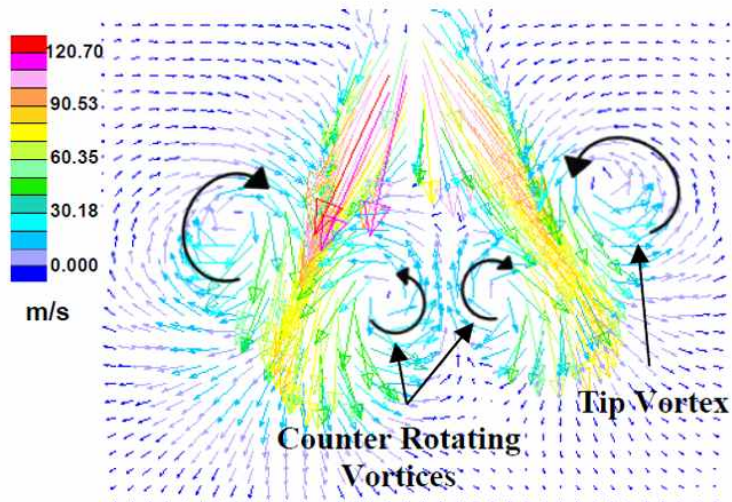


Figure 4.8 Velocity field around the flash-boiling sprays [9]

4.3. Spray characteristics according to the bio-alcohol concentration

Figure 4.9 shows the spray geometry according to the bio-alcohol concentration in three background conditions corresponding to real GDI engine operating conditions. It can be seen that the degree of flash-boiling was dependent on the alcohol content, and the flash-boiling occurred most strongly with the EB 30 mixture. This phenomenon is caused by the vapor pressure and boiling point change of fuel according to the evaporation ratio.

Alcohol has much lower vapor pressure than sub-octane gasoline, so it is expected that the vapor pressure of the mixed fuel will be lower than that of gasoline when alcohol is mixed with gasoline. However, blending alcohols into gasoline causes an increase in vapor pressure at low concentrations. The initial vapor pressure according to the alcohol concentration from the reference [10] and the measured values of our tested fuel are depicted in figure 4.10. This phenomenon is due to the fact that the blended fuel does not actually form an ideal solution but forms a non-ideal solution by intermolecular interaction between alcohols and gasoline molecules. For example, gasoline molecules disrupt the attractive forces such as hydrogen bond between alcohol molecules, and the repulsive force acts more dominantly between alcohol and gasoline molecules. However, when considering the initial vapor pressure of blended fuel only, EB 6 mixture should flash-boil the best. Therefore, it was required to

consider other theories to explain the best occurrence of vaporization in the EB 30 mixture.

It can be considered as an additional basis that the vapor pressure changes every moment as evaporation proceeds because the composition of the fuel changes during the evaporation. The boiling point of the gasoline increases as the evaporation progresses, while the boiling point of ethanol and butanol almost constant as shown in Figure 4.11. Especially when gasoline first begins to vaporize, the boiling point is lower than alcohol, and from a certain point onwards, the boiling point of gasoline is higher. Therefore, as shown in Figure 4.12, the temperature of blended fuel at 10 % distillation, which is close to the start of boiling, has risen with increasing alcohol content because the boiling point of gasoline is lower than alcohol. At lower alcohol content ratios, it seemed to be a bit lower for the same reasons as intermolecular interactions. Obviously, however, it was observed that the 50 % distilled point dropped as the alcohol content increases. This means that the fuel evaporates slower as the concentration of bio-alcohol increase, while the evaporation becomes faster as the concentration of bio-alcohol increase after some portion of the fuel distilled.

In summary, it was expected that the order of vapor pressure of blended fuel according to the alcohol content would be reversed as the evaporation proceeds. Although there is no exact distillation curve measured for the fuel actually tested, the phenomenon that the vapor pressure is reversed as the vaporization occurs has been studied in

the case of mixing only ethanol as shown in Figure 4.13 [11]. Therefore, EB30 fuel with an intermediate tendency is considered to be the most evaporative since the two effects of initial vapor pressure and vapor pressure change on mixture are combined.

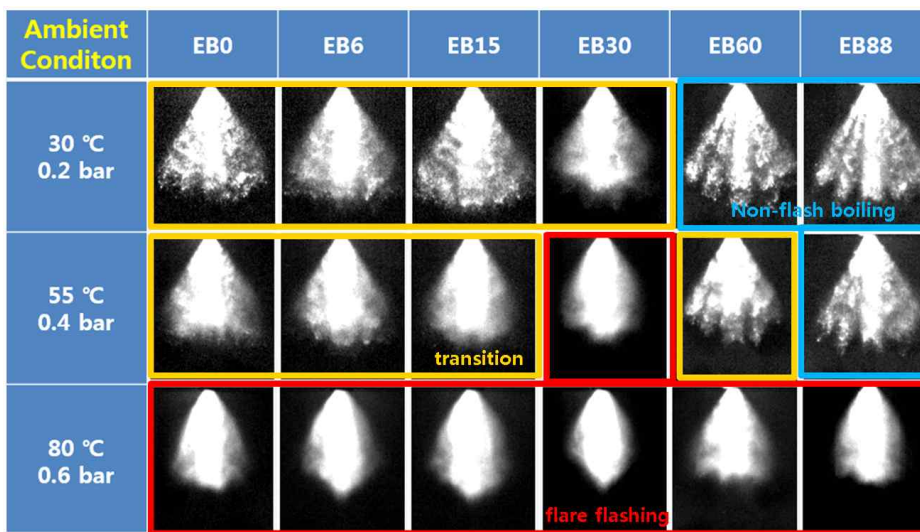
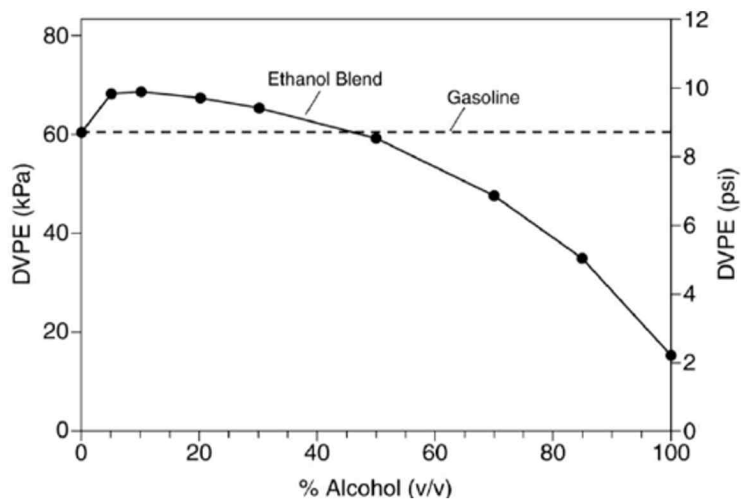
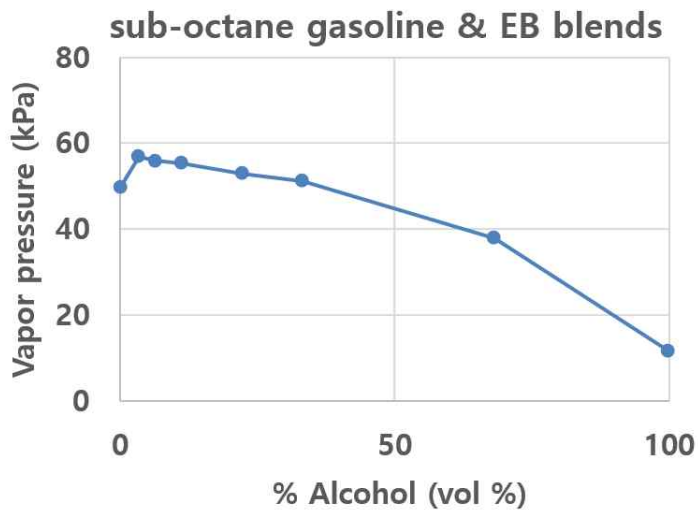


Figure 4.9 Spray images at engine operating conditions according to the bio-alcohol concentration (@ aSOI 0.7 ms)



(a)



(b)

Figure 4.10 (a) Vapor pressure of ethanol blend in gasoline with different relative proportions of ethanol by reference [10], (b) Vapor pressure of tested fuel measured by K-Petro (at 37.8 °C)

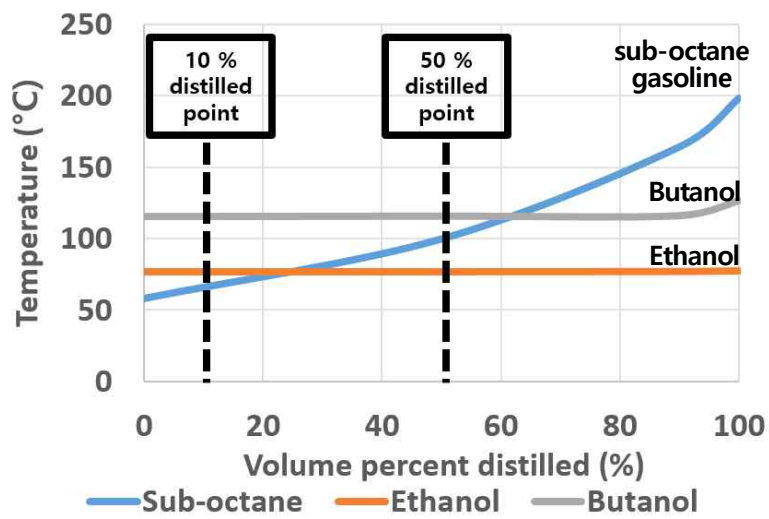


Figure 4.11 Boiling temperature according to the distilled ratio of each fuel

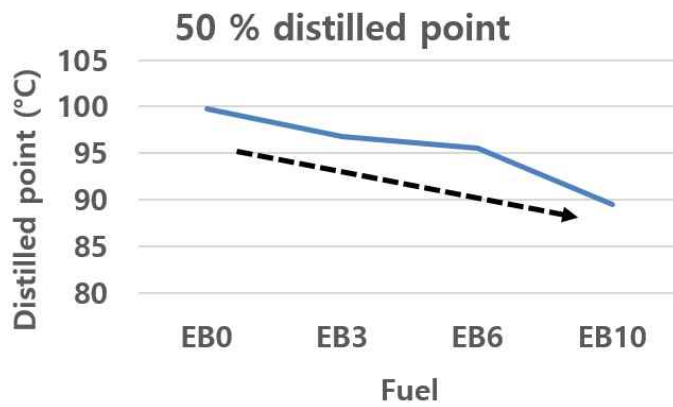
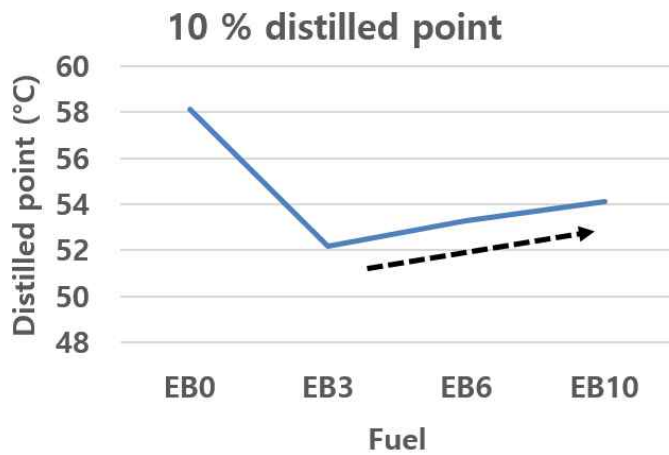


Figure 4.12 10 % and 50 % distilled point according to the alcohol concentration

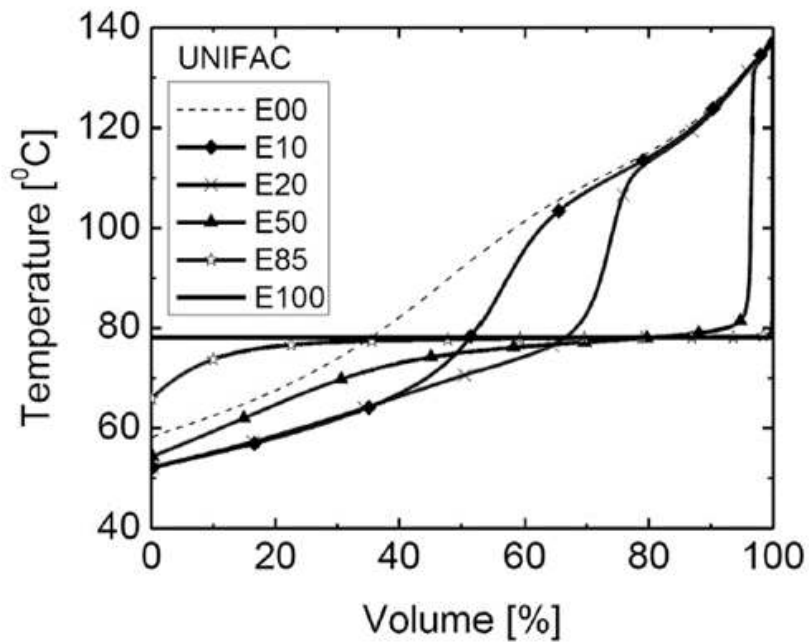


Figure 4.13 Predicted distillation curves for blends of ethanol and gasoline with non-ideal mixtures [11]

In chapter 4.3.1, 4.3.2, and 4.3.3, quantitative analysis of how penetration length and projected area change due to this phenomenon was discussed.

4.3.1. Results at low background temperature and pressure

At the background temperature and pressure condition of 30 °C and 0.2 bar, the low concentration of bio-alcohol increased the evaporation rate. The spray shapes of EB 0 to EB 30 corresponded to the shapes of the transition region, while the spray shape of EB 66 and EB 80 was corresponded to the non-flash-boiling shape because the evaporation rate was low. As the flash-boiling progresses, both spray area and penetration length decreased as shown in Figure 4.14. Especially, EB 30 mixture has the shortest penetration length because the flash-boiling occurred most in EB 30.

4.3.2. Results at middle background temperature and pressure

At the background temperature and pressure condition of 55 °C and 0.4 bar, the flash-boiling phenomenon became stronger than the 30 °C and 0.2 bar condition. It was observed that the EB 30 was the most evaporative fuel, and the front and rear fuels were in the transition zone, and EB 88 was still in the non-flashing zone. Especially, in the case of EB 30, the spray shape corresponded to the flare-flashing zone so that the penetration length was rather increased to about the length of EB 88 in the non-flashing zone as shown in Figure 4.15

due to the formation of the single plume.

4.3.3. Results at high background temperature and pressure

At the background temperature and pressure condition of 80°C and 0.6 bar, the flare-flashing occurred at all conditions of bio-alcohol concentration. Therefore, the spray area was similar in all conditions as shown in Figure 4.16. Penetration length was also found to be similar between the fuels but slightly increased as flare-flashing became stronger. In addition, the curvature of projected area and penetration length of spray was shown almost linear.

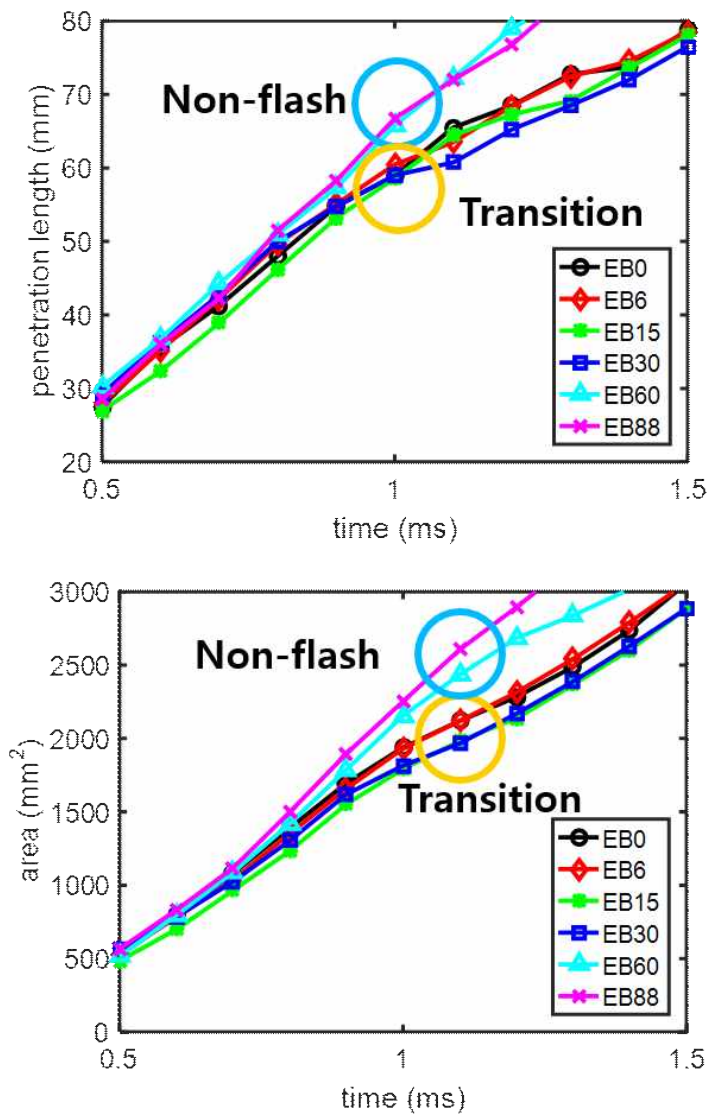


Figure 4.14 Penetration length and projected area of spray at background condition of 30 °C and 0.2 bar

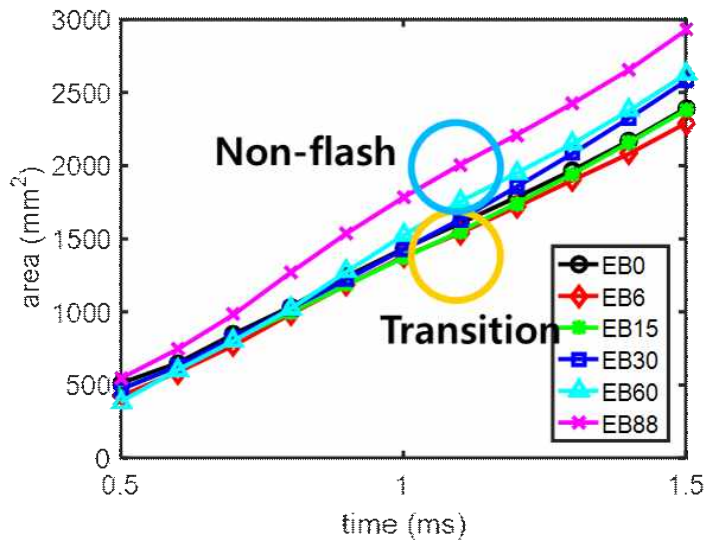
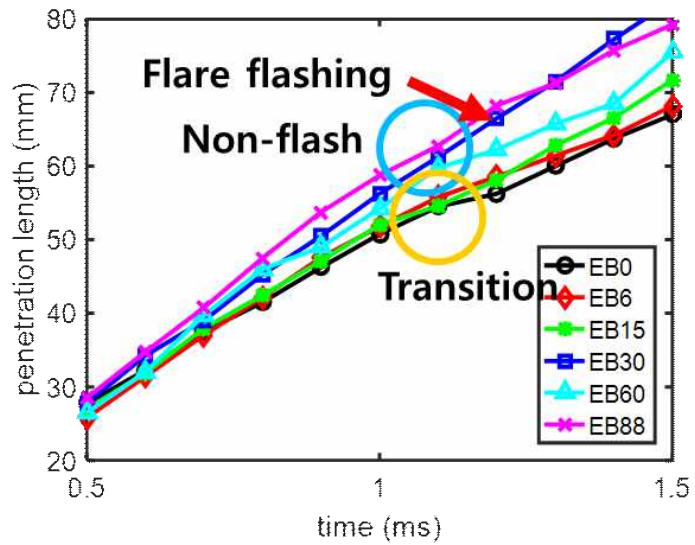


Figure 4.15 Penetration length and projected area of spray at background condition of 55 °C and 0.4 bar

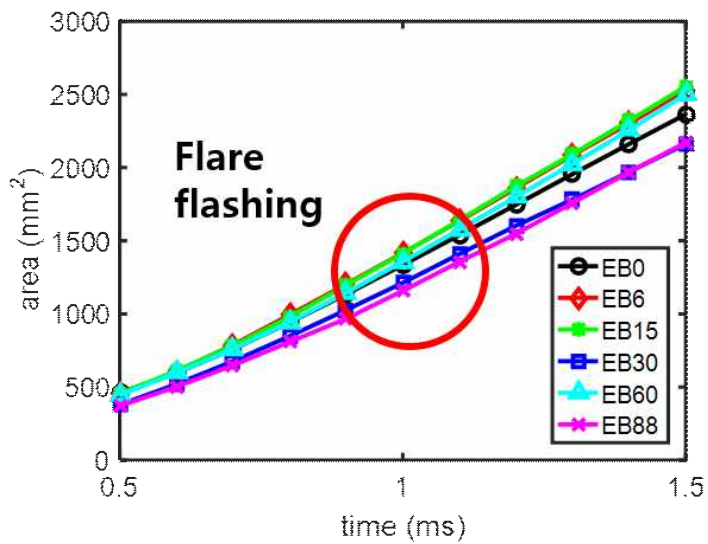
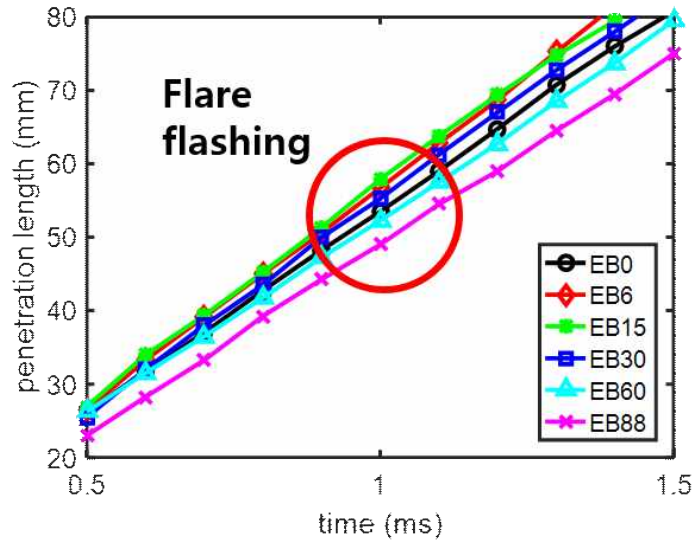


Figure 4.16 Penetration length and projected area of spray at background condition of 80 °C and 0.6 bar

5. Conclusion

In this study, spray experiments of blended fuels of sub-octane gasoline, bio-ethanol, and bio-butanol were performed in the real GDI engine operating conditions, and there were some points to be noted.

1. From the results, the operating range of the GDI engine included in the transition region in terms of flash-boiling, so the spray geometry changes most actively by flash-boiling.

2. When considering the concentration of bio-alcohol, flash-boiling occurred most strongly with the EB30 mixture due to vapor pressure and vapor pressure change of fuel according to the distilled ratio of the fuel mixture. Additional study on the distillation properties depending on the bio-alcohol concentration is suggested for accurate analysis of this phenomenon.

3. The effects of bio-alcohol concentration and flash-boiling on projected area and penetration length were different according to the background pressure (0.2, 0.4, 0.6 bar) and temperature (30, 55, 80 °C). As the flash-boiling phenomenon becomes stronger, the penetration length gradually decrease. However, the penetration length becomes longer at background condition of 0.6 bar and 80°C due to the formation of a single plume in the area where flare-flashing occurs.

References

1. International Energy Agency, (2015), Energy and Climate Change - World Energy Outlook Special Report, Available at: <https://www.iea.org/> [Accessed December 2018].
2. Simon Müller, Adam Brown, and Samantha Ölz, (2011), Renewable Energy: Policy Considerations for Deploying Renewables, International Energy Agency.
3. REN21, (2018), Renewables 2018 Global Status Report, Available at: <http://www.ren21.net/> [Accessed December 2018].
4. J. Serras-Pereira, P. G. Aleiferis, D. Richardson and S. Wallace, (2008), Characteristics of Ethanol, Butanol, Iso-Octane and Gasoline Sprays and Combustion from a Multi-Hole Injector in a DISI Engine (No. 2008-01-1591), SAE Technical Paper.
5. Francesco Catapano, Paolo Sementa, and Bianca Maria Vaglieco, (2016), Air-fuel mixing and combustion behavior of gasoline-ethanol blends in a GDI wall-guided turbocharged multi-cylinder optical engine, Renewable Energy, Vol. 96, Part A, pp. 319-332.
6. J. Senda, Y. Wada, D. Kawano, and H. Fujimoto, (2007), Improvement of combustion and emissions in diesel engines by means of enhanced mixture formation based on flash boiling of mixed fuel, International Journal of Engine Research, Vol. 9, Issue 1, pp. 15-27.
7. D. Kawano H. Ishii H. Suzuki, Y. Goto, M. Odaka, and J. Senda, (2006), Numerical study on flash-boiling spray of multicomponent fuel, Heat transfer-Asian research, Vol. 35, Issue 5,

pp. 369–385.

8. Wei Zeng, Min Xu, Gaoming Zhang, Yuyin Zhang, and David J. Cleary, (2012), Atomization and vaporization for flash-boiling multi-hole sprays with alcohol fuels, *Fuel*, Vol. 95, pp. 287–297.
9. Christopher Price, Arash Hamzehloo, Pavlos Aleiferis, and David Richardson, (2015), Aspects of Numerical Modelling of Flash-Boiling Fuel Sprays (No. 2015-24-2463), SAE Technical Paper.
10. V. F. Andersen, J. E. Anderson, T. J. Wallington, S. A. Mueller, and O. J. Nielsen, (2010), Vapor Pressures of Alcohol–Gasoline Blends, *Energy & Fuels*, Vol. 24, Issue 6, pp. 3647–3654.
11. Jiao, Q., Ra, Y., and Reitz, R., (2011), Modeling the Influence of Molecular Interactions on the Vaporization of Multi-component Fuel Sprays (No. 2011-01-0387), SAE Technical Paper.

요약

광학 계측법을 이용한 서브옥탄 가솔린과 바이오 에탄올/부탄올 혼합연료의 GDI 분사 특성 연구

서울대학교 대학원

기계항공공학부

민형은

운송부분에서의 이산화탄소 배출량을 줄이고 가솔린 연료의 옥탄가를 높이기 위한 방안으로 가솔린에 바이오 연료를 혼합해 사용하는 것이 제안된 바 있다. 본 연구에서는 서브옥탄 가솔린에 에탄올과 부탄올의 구성비가 7:3인 바이오 알코올을 혼합한 연료의 분사 특성을 실제 GDI 엔진 운전 조건에서 분석하였다. 분사 배경 조건은 정적 연소실을 이용하여 모사하였으며, 미 산란 기법과 솔리렌 기법을 이용해 스프레이 가시화를 수행하였다. 이를 통해 바이오 알코올 혼합비에 따라 총 6종의 연료(EB 0, 6, 15, 30, 60, 88)의 분사 특성을 비교 분석하였다. 그 결과, GDI 엔진 운전 조건이 플래시보일링 관점에서 전이 영역에 주로 위치하고 있으며, 플래시보일링 발생 정도에 따라 스프레이 형상이 크게 변화

하는 것이 확인되었다. 플래시보일링 발생 정도는 알코올 함량에 따라 변화하는데, 특히 EB30 연료에서 플래시보일링이 가장 강하게 일어나는 것이 관측되었다. 이를 알코올 혼합에 따른 초기 증기압 변화와, 분사 후 증발에 의한 혼합 연료의 구성비 변경에 따른 증기압 변화로 해석하였다. 배경 온도와 압력에 따라 바이오 알코올 혼합 연료의 스프레이 침투 거리와 투영 면적을 정량 계측하였으며, 플래시보일링이 강하게 발생하여 단일 플룸이 형성되는 현상이 스프레이 특성에 미치는 효과를 고찰하였다.

주요어: 바이오 알코올, 바이오 혼합연료, GDI 스프레이 특성,
플래시보일링, 미 산란 기법

학번: 2014-21850